Experimental Thermal and Fluid Science 81 (2017) 93–108

Contents lists available at ScienceDirect

Experimental Thermal and Fluid Science

journal homepage: www.elsevier.com/locate/etfs

Experimental investigation on the initiation and flow development of gas-liquid slug two-phase flow in a horizontal pipe

Okto Dinaryanto [a,c], Yosephus Ardean Kurnianto Prayitno [a,b], Akmal Irfan Majid [a,b], Akhmad Zidni Hudaya [a,d], Yusnanda Agus Nusirwan [a], Adhika Widyaparaga [a,b], Indarto [a,b], Deendarlianto [a,b,*]

[a] Department of Mechanical & Industrial Engineering, Faculty of Engineering, Universitas Gadjah Mada, Jl. Grafika No. 2, Yogyakarta 55281, Indonesia
[b] Center for Energy Studies, Universitas Gadjah Mada, Sekip Blok K 1A, Yogyakarta 55281, Indonesia
[c] Department of Mechanical Engineering, Sekolah Tinggi Teknologi Adisutjipto, Blok R Lanud Adisutjipto, Yogyakarta 55198, Indonesia
[d] Department of Mechanical Engineering, Universitas Muria Kudus, Kampus Gondangmanis, Kudus, Central Java, Indonesia

ARTICLE INFO

Article history:
Received 20 June 2016
Received in revised form 30 September 2016
Accepted 12 October 2016
Available online 13 October 2016

Keywords:
Slug initiation
Slug flow development
Visual observation
Pressure fluctuations
Slug initiation frequency

ABSTRACT

Slug flow is the most prevalent problem of two-phase fluid transportation in the petroleum industries. Here, large amplitude waves lead to the pipe blockage that possible to cause the damage of the mechanical structure. The experimental investigation of gas-liquid slug two-phase flow in a horizontal pipe was carried out to investigate the initiation and flow development mechanisms. Air and water were used as the working fluids. The inner pipe diameter was 26 mm. In the present experimental study, the slug initiation mechanisms were explained by visual observation and pressure fluctuations. Moreover, the initiation frequency of slug flow and the evolution of passing slug frequency along the pipeline were also observed by using two high video cameras.

As a result, several basic mechanisms of slug flow initiation in a horizontal pipe were clarified. Those were the wave coalescences, the wave growth mechanism, and the large disturbance waves. A flow initiation map was proposed to address those mechanisms. Here, the slug initiation frequency and the passing slug frequency were obtained in relation to the pipe length position. The static pressure measurement was also used to verify the image processing results on the characteristics of slug initiation mechanisms. The obtained qualitative and quantitative results from the investigation can be used to evaluate the recent available models.

1. Introduction

Two-phase flow phenomena are often encountered in various industrial applications such as petroleum, process, and power plant. One of the most dangerous cases, namely as the slugging phenomena, should be avoided due to the existence high oscillation pressure inside the pipe and produces a high vibration on the piping structure. Due to the momentum of the slug flow, vibration and mechanical forces should be considered to ensure the operational safety and the design of the pipeline system. The fluctuating liquids and the gas slugs induce the structural disadvantages that lead to crack and corrosion of the pipe [26]. Furthermore, the high frequency slug flows speed up the pipe corrosion rates [1]. From the view point of multiphase flow, the understanding of the slug initiation mechanism is very important in pipeline design.

Slug flow is generated when the gas flow increases and the liquid slugs move downstream with highly aerated unsteady fronts. Prior to the appearance of these phenomena, a stratified flow occurs at lower gas flow rates and lower liquid flow rates. Then, when the gas flow rates increase, a stratified wavy flow is formed. Furthermore, at higher liquid flow rates, waves appear at the interface and may reach the top of the pipe and form the liquid plugs that separated by large gas bubbles, which is known as a plug flow [10]. Next, when the gas flow increases at high liquid flow rates, a slug flow exists.

The wave growth mechanisms have been proposed by many researchers in the previous studies. Taitel and Dukler [22] described the classical model of Kelvin-Helmholtz instability theory to develop the wave growth mechanism for inviscid fluid, known as the Inviscid Kelvin-Helmholtz (IKH). However, applying this theory for all slug flow cases face a shortcoming especially on the assumption of an ideal fluid with no viscosity. A study

* Corresponding author at: Department of Mechanical and Industrial Engineering, Faculty of Engineering, Gadjah Mada University, Indonesia.
E-mail address: deendarlianto@ugm.ac.id (Deendarlianto).

http://dx.doi.org/10.1016/j.expthermflusci.2016.10.013
0894-1777/

conducted by Lin and Hanratty [14] addressed a better prediction by using viscous fluid to develop the slug mechanism based on the analysis of Viscous Long Wavelength (VLW) instability. Their study also involved the influence of shear stress on the pipe wall that was not observed in the study by Taitel and Dukler [22]. At his point, two general models mentioned above have been carried out to define slug flow formation.

Currently, the slug stability theorem is used to predict the onset of slug flow. It considers the importance of liquid attached rates at the front and its shedding from the rear of slug flow. Slugs are stable if the rates of liquid attached are same as the rates at which the liquid's sheds [10]. This theory is used to predict the critical liquid height for the development of slug flow whereas the slug stability analysis consider a volumetric liquid balance between the front and the tail of a slug, as mentioned by Andritsos et al. [3], Andreussi et al. [2], Ruder et al. [18], Soleimani and Hanratty [21], Woods and Hanratty [28], and Woods and Hanratty [29]. This concept explains a parameter for a stable slug flow in the high superficial velocities. Nevertheless, it did not explain the formation of slug flow in detail and there is still a lack of accurate studies which address comprehensively on slug initiation mechanism from the visual observation and pressure characteristics. Hence, an experimental study is essentially needed to provide high quality experimental data that able to clarify a better understanding of slug initiation mechanism [5].

Although many scholars (Mishima and Ishii [16], Ruder et al. [18], Zhang et al. [31], Soleimani and Hanratty [21], Taitel and Dukler [22], Ujang et al. [25], Hanyang and Liejin [9], Sanchis et al. [19], and Nieckele et al. [17]) have studied the slug formation mechanisms, there are limited studies on slug flow characteristics where the slug is initiated and developed. Woods and Hanratty [29] divided the slug initiation models into three zones based on the Froude number, manifested in a flow initiation map for the case of 76.3 mm inner pipe diameter. On the other hand, Lin and Hanratty [13] revealed the "pseudo-slug" concept for the air-water flow with large amplitude waves that failed to form a liquid blockage. They also mentioned that slug formation is influenced by Kevin-Helmholtz (wave growth) and wave coalescence models which are depended on gas and liquid velocities. On the other hand, Mishima and Ishii [16] developed a theoretical prediction of onset of horizontal slug flow. Fan et al. [7] proposed four basic mechanisms for the onset of slugging on the basis of wave behavior inside a horizontal pipe with the inner diameter of 95 mm. On the other hand, Ujang et al. [25] conducted the air-water slug initiation and flow development inside a pipe with inner diameter of 78 mm by using conductance probes. However, most of the above mentioned studies were conducted in large pipe diameter. Also, the studies on the distribution of slug frequency in the initiation area and the spatial data of slug frequency along the length of pipe has not been reported so far. Thus, it is essential to conduct a study for revealing the slug initiation and evolution inside the intermediate pipe diameter.

Slug frequency is also important subjects to address the slug flow characteristics. In practical applications, the slug frequency is proportional to the pipeline structural damage, corrosion rate, and coating protection of the pipe [1,24]. Slug frequency has been previously discussed by the scholars, among them were Taitel and Dukler [23], Fan et al. [7], Woods et al. [30], Ujang et al. [25], Wilkens et al. [27], and Al-Safran [1]. To prevent the pipe structural damage due to slug flows, the observation on reason, timing, and characteristics of the occurred slugs become essential. However, the studies on the slug initiation in the relation of the pipe position were not considered so far. A relationship between slug initiation and the frequent position where they are initiated (initiation area) can be an interesting subject to be investigated. By recognizing where the slug flows frequently appears, the maintenance system can be assisted, for example by installing a slug catcher or performing a particular treatment. Therefore, it is necessary to investigate slug initiation frequency and the evolution of the passing slug frequency along the pipeline.

The aim of the present work is to investigate the initiation process and the development of slug flow inside a horizontal pipe. The inner pipe diameter was 26 mm. As the rapid development of CFD codes, high quality experimental data (in temporal and spatial) to validate the code itself are essentially needed [4]. This work is dedicated also to support the theoretical model development and validation of CFD codes by high quality temporal and spatial experimental data of air-water slug flow. To achieve the comprehensive results, this present study involves the simultaneous observation of the visual observation and the pressure measurement. Moreover, a better understanding of the slug initiation process and slug flow development, obtained from the present experimental study, are essential for the evaluation of the available models.

2. Experimental apparatus and procedure

A schematic diagram of the experimental apparatus is shown in Fig. 1. The experiments were carried out at Horizontal Two-Phase Flow Facility (HORTOFF) of the Fluid Mechanics Laboratory, Department of Mechanical and Industrial Engineering, Universitas Gadjah Mada, Indonesia that was also previously used. It was made of a 10 m length of acrylic pipes, with an internal diameter of 0.026 m. The length of the test section is designed for 0–210 D or around 5.46 m to ensure the slug flow is well developed. Moreover, the length after the test section is designed for 210–385 D or around 5.54 m to ensure the oscillation that occurred at this section will not harm on the test section. To ensure the uniformity of wall roughness, the same materials for the entire pipe were used. In addition, before conducting the experiments, the ends of each tube and the flange were smoothly machined to provide smooth junctions. The connections between the tubes were also machined to maintain the smoothness in the whole pipeline and minimize the gaps.

In the present study, the experiments were conducted under room temperature where the air was supplied from a compressor at the maximum amount of 600 LPM and pressure of 8 bars (gauge). The air regulator was equipped with constant pressure, to ensure a constant inlet pressure. To control the air flow rate, two *Dwyer* gas rotameters with maximum capacities of 200 and 600 standard cubic feet/minute, and approximately 3% accuracy were used. To supply the water, a centrifugal pump, which has a minimum fluctuations compared to other pump types, with a capacity of 18 m^3/h, was used. A flexible hose was also installed at around inlet area to reduce the flow oscillations and vibrations. Here, two *Omega* water rotameters with maximum capacities of 10 GPM and approximately 2% accuracy were used in order to control the water flow rates.

The facility is also supported by the measuring devices to observe the flow behavior and to measure the pressure on the specific locations. The observations were conducted at the specific points of 25 D (Diameter), 50 D, 75 D, 100 D, 150 D, 180 D, and 210 D from the inlet. To observe the flow development and the slug frequency along the pipe, two high-speed video cameras with maximum frame rate of 1200 fps were used. The first and second full HD cameras have a maximum resolution of 3000×4000 pixels and 1920×1080 pixels respectively. Both cameras were used simultaneously in different coverage area in order to observe the flow behaviors and the slug frequency during 120 s. The first camera covered the observation of the flow behavior in the initiation area, 25–75 D, while the second camera was used to observe the

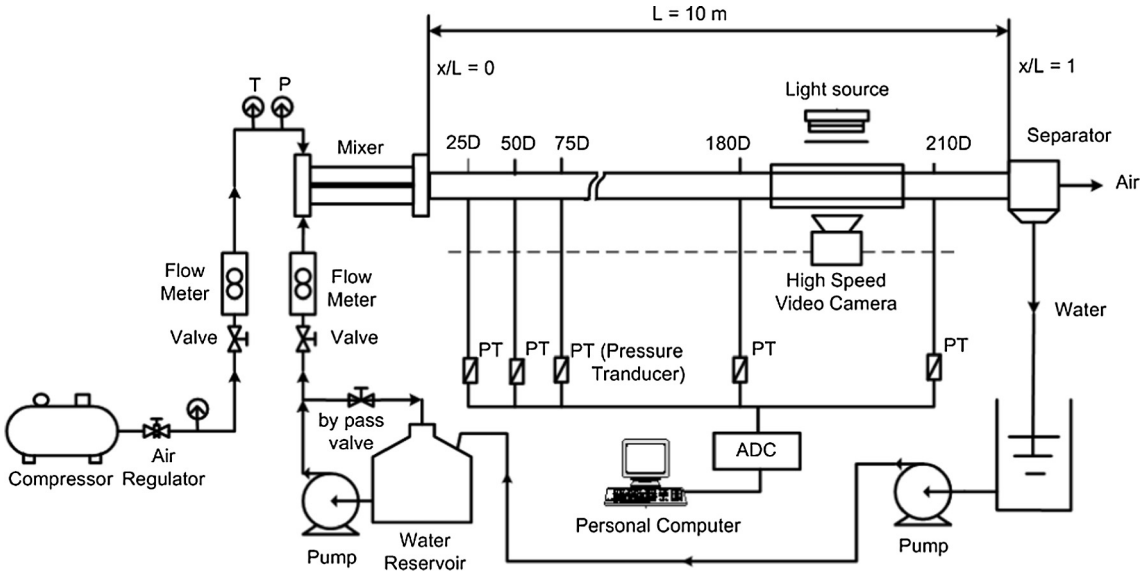

Fig. 1. Schematic diagram of the experimental apparatus.

flow behavior in the developed area, 180–210 D (developed area). Hence, the spatial results of the visualization studies could be obtained. Series of LED lamps were used as the lighting sources to support the visualization study. To reduce the image distortion of air-water flows inside a tube, a correction box is needed to minimize the difference in refractive indices between the fluids and tube wall material, as indicated by Kawahara et al. [11]. A rectangular transparent acrylic box was installed at the developed flow test section, about 5 m from the water and gas inlet, which is used to reduce the image distortion during the observations. The correction box was filled by water that had an almost similar to acrylic's refractive index to enhance the visualization observation. Thus, the phenomenon occurred in the near wall would be magnified and the details of the two-phase slug flow behavior could be better investigated.

The recorded video and images were then analyzed by using the image processing technique to obtain the visualization data. To verify the visualization data, the static pressure measurements were carried out. The measurement of static pressure fluctuations used Validyne® pressure transducer which was located on five positions: 25 D, 50 D, 75 D, 180 D, and 210 D. The pressure transducers were installed at the bottom surface of the pipeline and connected to the data acquisition and personal computer. The pressure transducers specifications were 0–56 kPa (g) and 0–86 kPa (g). The pressure gradient between two locations was also measured by the Validyne® pressure transducer with the full-scale uncertainty level of 0.25%. Furthermore, the recorded static pressure was obtained by Easysense 2250-Validyne® software with 500 data/s during 120 s observation. Based on, the static pressure measurement, the fluctuating pressure, caused by the presence of slug at the specific location can be identified.

A specific configuration of the water and air inlet was installed to keep the air and the water flow separately into the test section, as illustrated in Fig. 2. The air was supplied to the inlet from the top section and water entered from the bottom section. Based on the former experiments, to align the initial flow and modify the two-phase flow into a stratified flow which is suitable to study the slug flow initiation, a splitter plate was installed at the center area of the mixer as used by Ujang et al. [25]. The initial flow entered the pipeline from the initiation test section (from 25 D to 75 D) to the developed test section (from 180 D to 210 D). Here, the visualization studies were conducted at the initiation test section in order to investigate slug initiation mechanism, slug initiation position, and the evolution of slug frequency. At the test section where slug flow had been developed, visualization studies were performed to determine the slug flow-topography, especially during the stable condition.

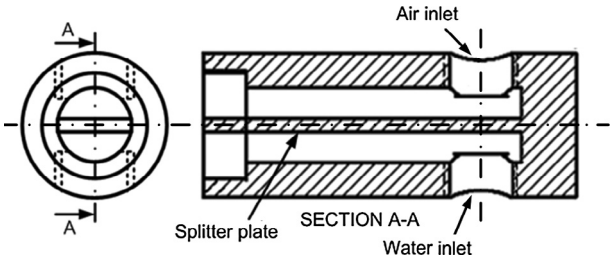

Fig. 2. Configuration of air-water mixer.

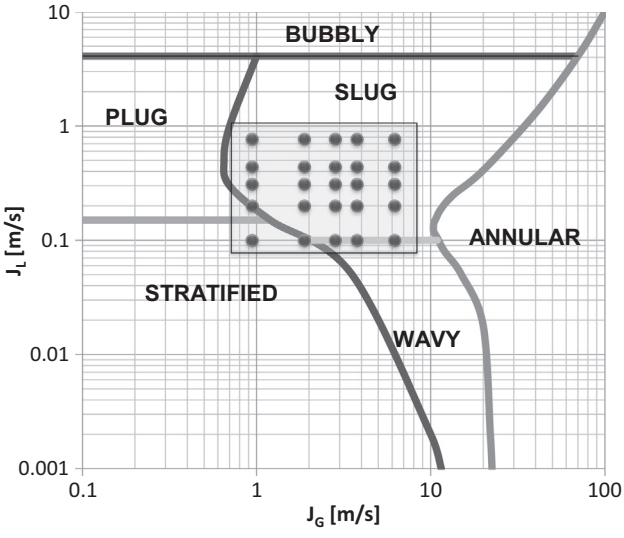

Fig. 3. Experimental data plotted on the Mandhane et al. [15] map.

The experimental conditions were plotted on the Mandhane flow pattern map, as shown in Fig. 3. The range of water and air superficial velocities: J_L = 0.10–0.77 m/s and J_G = 0.94–6.20 m/s, respectively. Experiments were conducted at atmospheric pressure and room temperature. The observations at the low liquid superficial velocities were conducted to investigate the presence of the first wave, second wave, and the pseudo-slug, firstly. At the higher liquid superficial velocities, observations were focused on the presence of the wave coalescence, the pipe blockage due to the growth of wave, the elongated bubble, the liquid slug, and its relation to the Kelvin-Helmholtz instability. Under the high liquid superficial velocities, the observations were aimed to investigate the irregular waves and the initiation positions of the slug flow.

3. Results and discussions

3.1. Visualization study

Visualization studies were carried out at the initiation flow test section (from 25 D to 75 D) and the developed flow test section (from 180 D to 210 D). From the experiments, the obtained flow patterns were stratified, pseudo-slug, and slug flow. However, the present study was focused on the slug flow mechanism including pseudo-slug and slug flow. Figs. 4–9 are the snapshot of the many distribution initiation at the initiation area. It shows the phenomenon of the pseudo-slug, wave coalescences and the developing slug flow. Moreover, Figs. 10–15 are the snapshots of the phenomenon at the developed area including the mechanism of developed slug flow.

At low J_L, slug flow rarely appeared. For J_L = 0.10 m/s the large waves appeared in the form of roll waves. The wave velocities differed among each other and causing wave coalescences. For J_G = 2.83 m/s, the wave coalescence was able to form a temporary blockage which then developed into a pseudo slug, as shown at t = 0.083 s in Fig. 4. Here, the pseudo-slug is defined as the disturbances which have the appearance of slugs, as previously stated by Lin and Hanratty [13]. However, when the J_G was increased to J_G = 6.20 m/s, the initially formed roll waves were more frequent but had smaller amplitudes. Therefore, the roll wave coalescence could not form a blockage due to insufficient liquid supply. The coalescence only resulted in formation of larger amplitude roll waves as shown in Fig. 5.

At a higher liquid superficial velocity (J_L), where J_L = 0.31 m/s, the waves were developed under the mechanisms of wave growth and wave coalescence. At J_L = 0.31 m/s and J_G = 1.88 m/s, the waves continued to grow and reached the top area of the pipe, as shown in Fig. 6. Hence, the onset of slug flow, identified by the liquid blockage, was clearly indicated at t = 0.017 s in this figure. Consequently, the blockage separated the large wave air-water flows into the consecutive elongated bubbles and the liquid slugs. Although the presence of the elongated bubbles and the liquid slugs could be identified, the leading and trailing elongated bubbles might still coalesce due to the waves growth.

When the J_G was increased at a constant J_L, where the combination of J_G = 6.20 m/s and J_L = 0.31 m/s as an example, the liquid was lifted by the gas flow to the upper cross-sectional area of the pipe and produced the irregular waves that flow rapidly to the developed flow test section. The increase of gas superficial velocity plays an important role to the velocity of the irregular waves and lead to the waves coalescences, as shown at t = 0.017 s in Fig. 7. At this stage, the liquid and gas phases mixed and the liquid slug contained tiny aerated bubbles, as shown at t = 0.067 s and t = 0.083 s in Fig. 7.

Under the high liquid superficial velocities ($J_L \geqslant 0.35$ m/s), specifically at J_L = 0.77 m/s, the slug occured more frequently than that at the lower J_L area. As shown in Fig. 8, in this region, the slug

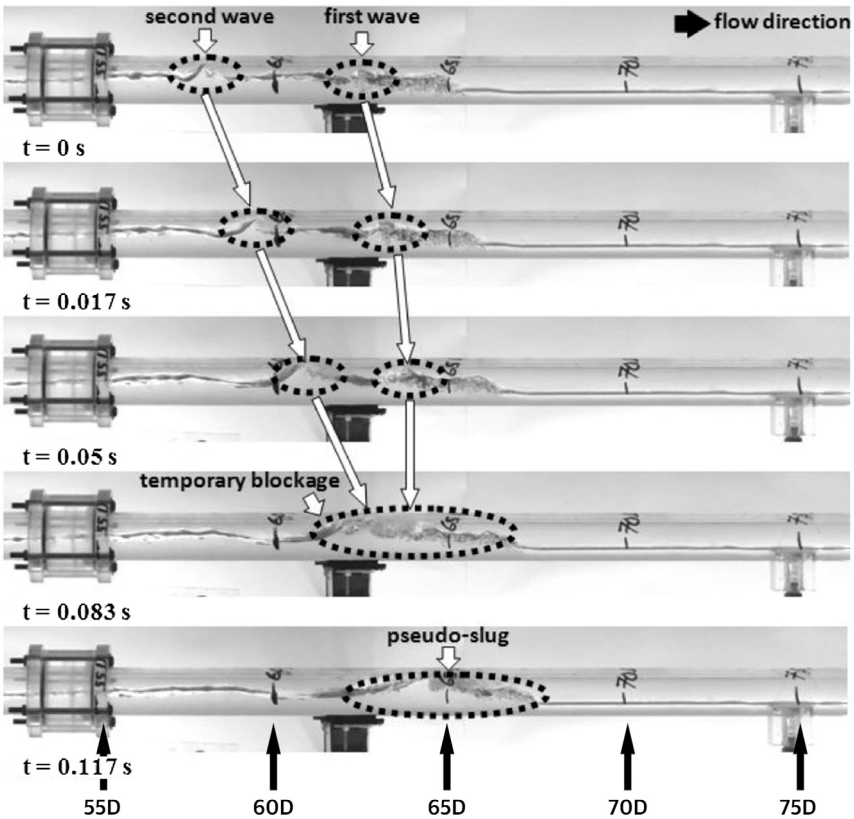

Fig. 4. Snapshot of the interfacial behavior of the pseudo-slug formation at initiation section 55 D–75 D (J_L = 0.10 m/s and J_G = 2.83 m/s).

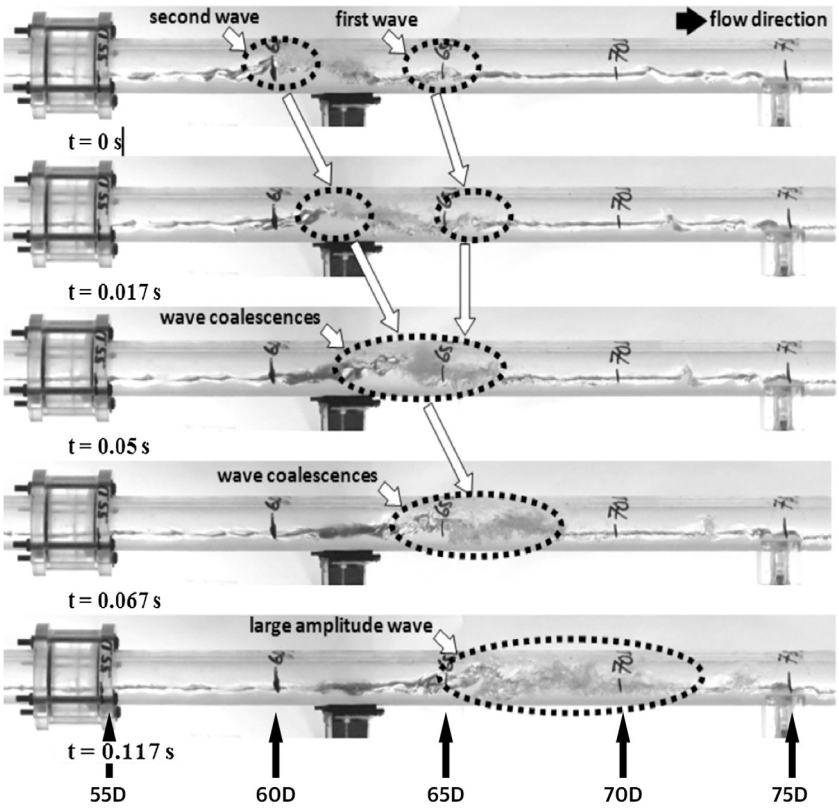

Fig. 5. Snapshot of the interfacial behavior of the roll waves coalescence mechanism at initiation section 55 D–75 D (J_L = 0.10 m/s and J_G = 6.20 m/s).

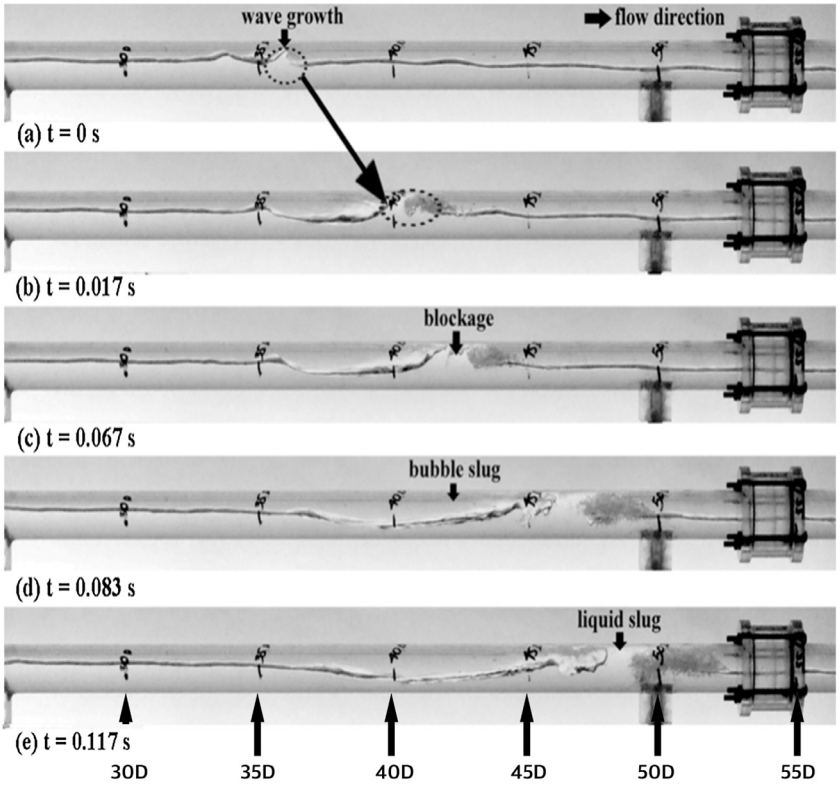

Fig. 6. Snapshot of the interfacial behavior of slug flow at initiation section 30 D–55 D (J_L = 0.31 m/s and J_G = 1.88 m/s).

flow initiation mechanism was still influenced by the wave growth. However, the disturbance waves were present and stimulated the slug flow initiation. As shown in Fig. 8, under low gas superficial velocities regions ($J_G \leqslant 3.00$ m/s), the slug mechanism was

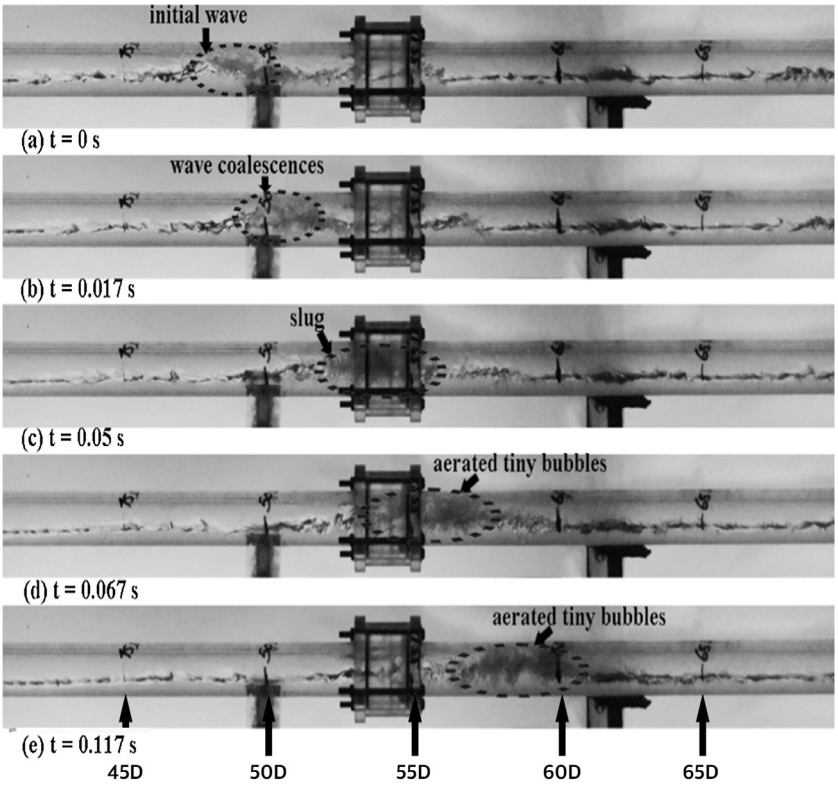

Fig. 7. Snapshot of the interfacial behavior of the slug flow initiation at initiation section 45 D–65 D (J_L = 0.31 m/s and J_G = 6.20 m/s).

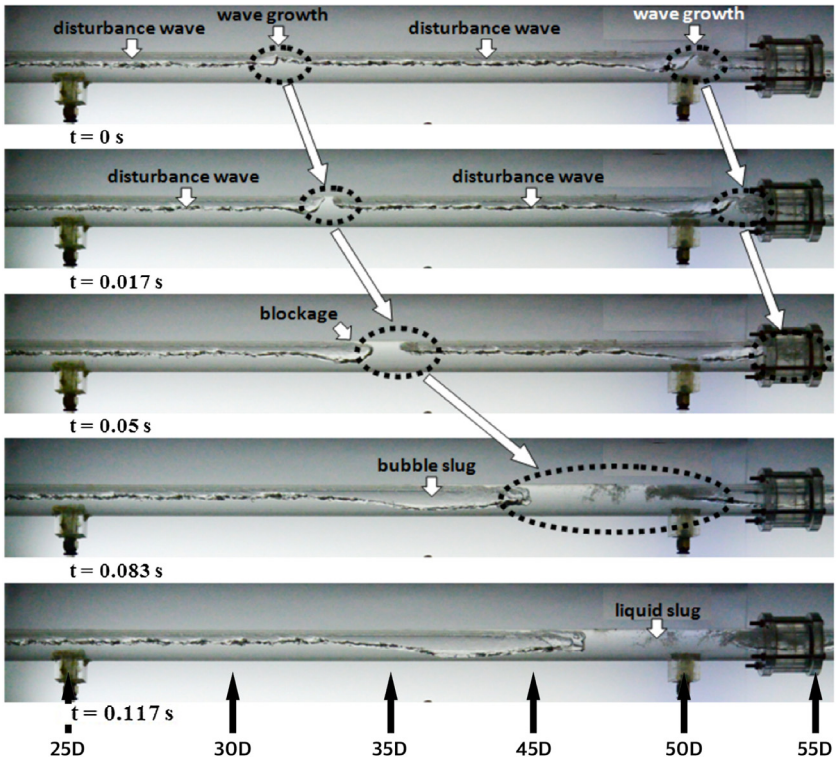

Fig. 8. Snapshot of the interfacial behavior of the slug flow initiation for high liquid flow at initiation section 25 D–55 D (J_L = 0.77 m/s and J_G = 1.88 m/s).

influenced by the wave growth and the disturbance waves. For the higher gas superficial velocities ($J_G \geqslant 3.00$ m/s) as shown in Fig. 9, the turbulence and water level at the water and air inlet location were high enough to stimulate the liquid blockage. The large interfacial disturbance near the inlet has a significant effect on the initiation of slugs. At this stage, the slug formation was initiated

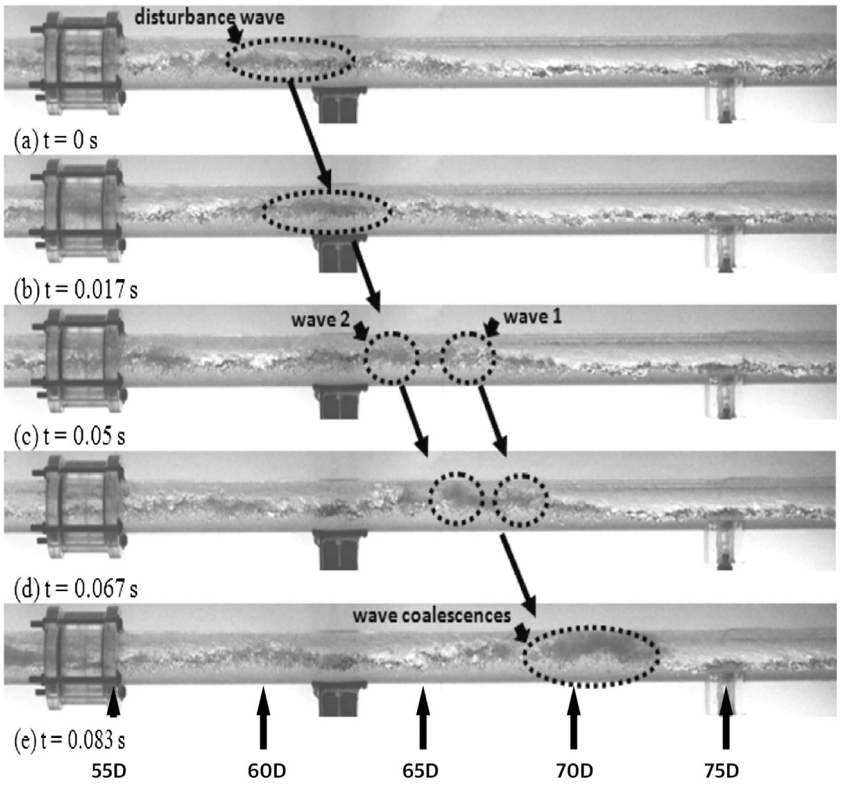

Fig. 9. Snapshot of the interfacial behavior of the slug flow initiation for high liquid flow at initiation section 55 D–75 D (J_L = 0.77 m/s and J_G = 6.20 m/s).

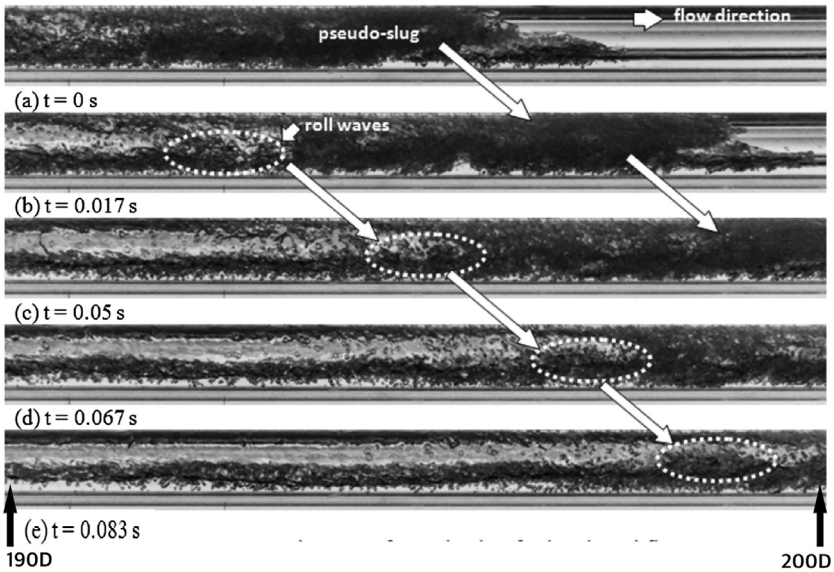

Fig. 10. Snapshot of the pseudo-slug visualization for low liquid flow at developed section 190 D–200 D (J_L = 0.10 m/s and J_G = 2.83 m/s).

by the disturbance waves and the wave coalescence. The observation results for the developed slug flow were shown in Figs. 10–15 for low, medium, and high liquid superficial velocities. At the low liquid superficial velocity (J_L = 0.10 m/s), the flow exhibited different characteristics for at low gas superficial velocity (J_G = 2.83 m/s) compared to high gas superficial velocity (J_G = 6.20 m/s). As shown in Fig. 10, at J_G = 2.83 m/s, the flow contains a high amount of dispersed bubbles. The liquid is insufficient to form a blockage in the pipe and turn into roll waves. The waves then collide with each other and form a pseudo slug which contains a high amount of dispersed bubbles. Next, as shown in Fig. 11, at J_G = 6.20 m/s, the pseudo-slug is not present. Instead, large amplitude waves exist. Nevertheless, the waves fail to form a slug flow despite colliding with each other.

At medium J_L, liquid slugs are present. For J_L = 0.31 m/s, a number of small bubbles increases and produce the dispersed bubbles at the bubble tail of the liquid slug, as shown in Fig. 12. However, under a higher gas superficial velocity, at J_G = 6.20 m/s, those dispersed bubbles at the bubble tail of the liquid slug develop in high amount. The majority of the liquid slugs turned into dispersed

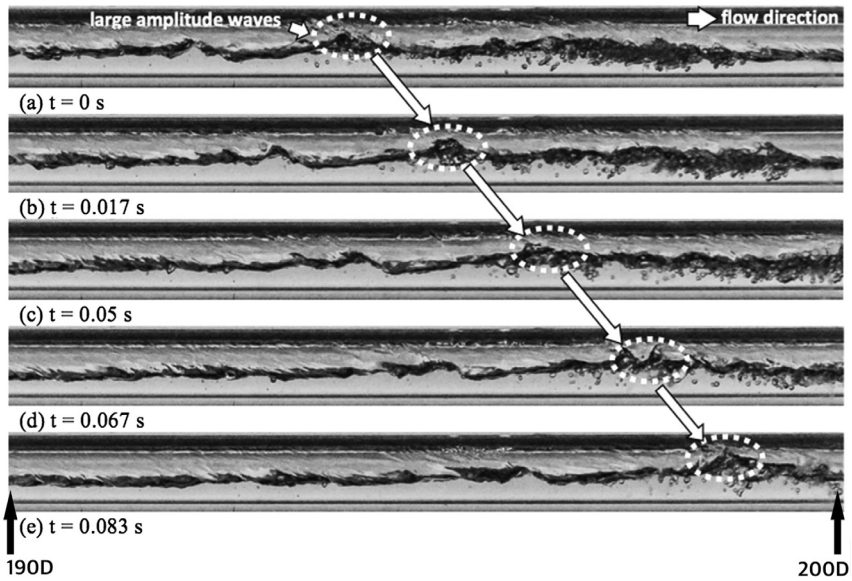

Fig. 11. Snapshot of the large amplitude waves visualization for low liquid flow at developed section 190 D–200 D (J_L = 0.10 m/s and J_G = 6.20 m/s).

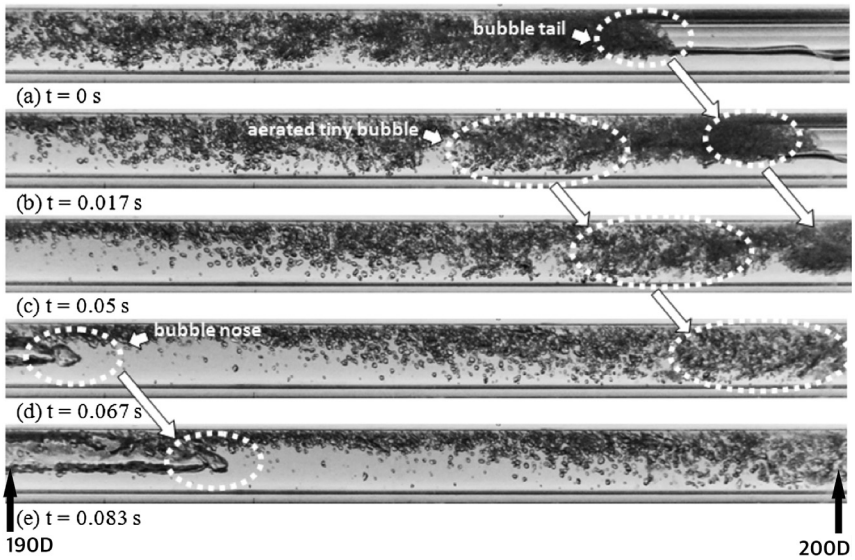

Fig. 12. Snapshot of the developed slug flow visualization for medium liquid flow at developed section 190 D–200 D (J_L = 0.31 m/s and J_G = 1.88 m/s).

bubbles due to the force of the gas. Fig. 13 indicates that the dispersed bubbles were dominantly presented at the surrounding of tail and elongated bubble.

It was known that the developed slug flows occur at the higher liquid superficial velocities when they reach constant length, identified by the equal tail and front velocities. Slug flow was initiated by the wave growth, the pipe blockage, and the presence of liquid slugs, followed by the gas slugs. During the flow development, slugs initially grow in length due to a velocity discrepancy between its tail and front area [25]. The observed flow development mechanisms in the study was in agreement. Slug flow was shown to develop and with longer distance from the inlet, the slug flow increasingly stabilized.

Fig. 14 shows the interfacial behaviors of slug flow at a high liquid superficial velocity, (i.e. J_L = 0.77 m/s). As explained before, the slug that occurs at the higher liquid superficial velocities approaches a constant length whereas the front and tail velocities are equal, as also indicated by Ujang et al. [25]. Meanwhile, at the high gas superficial velocity (J_G = 6.20 m/s), the dispersed bubbles occurred on the developed test section, as the consequences of the disturbance waves that appeared at the initiation test section. Fig. 15 shows that the existence of dispersed bubbles become more dominant as the J_G increases. A highly aerated slugs exist as the high gas velocity induces a higher interfacial shear.

To conclude the obtained results from the visual observation, the mechanism of slug flow formation in relation to J_L and J_G is described in Fig. 16. The proposed map is described as the function of gas and liquid superficial velocities. At the low J_L and high J_G, slug flow is rarely formed during the observation, addressed as Region I. For the low gas superficial velocities ($J_G \leqslant 3.00$ m/s), the large waves are developed under the wave growth mechanism, addressed as Region II. As the J_L increases, the slug flow is initiated by the presence of wave growth and the disturbance waves, addressed as the Region III. On the other hand, the high gas superficial velocities ($J_G \geqslant 3$ m/s) area was addressed as the Region IV where slug flow is initiated by the wave coalescence and the

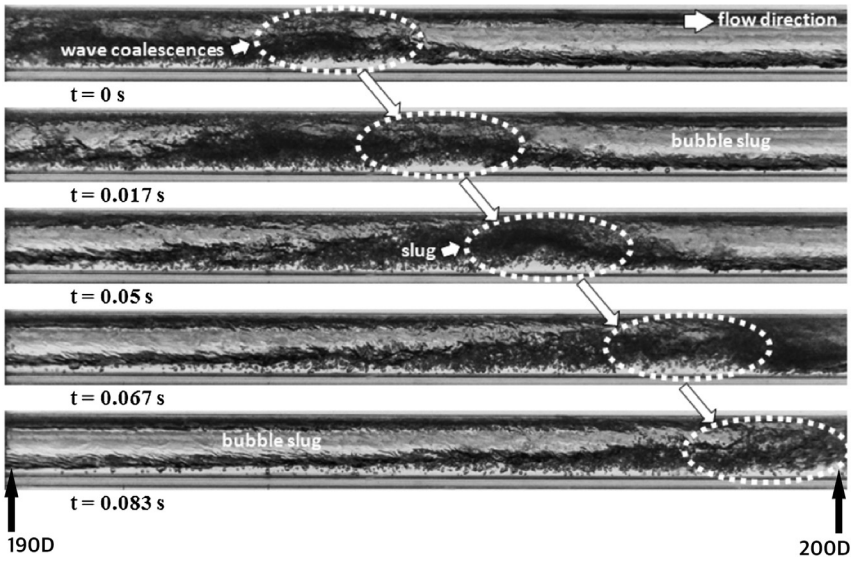

Fig. 13. Snapshot of the slug flow visualization for medium liquid flow at developed section 190 D–200 D (J_L = 0.31 m/s and J_G = 6.2 m/s).

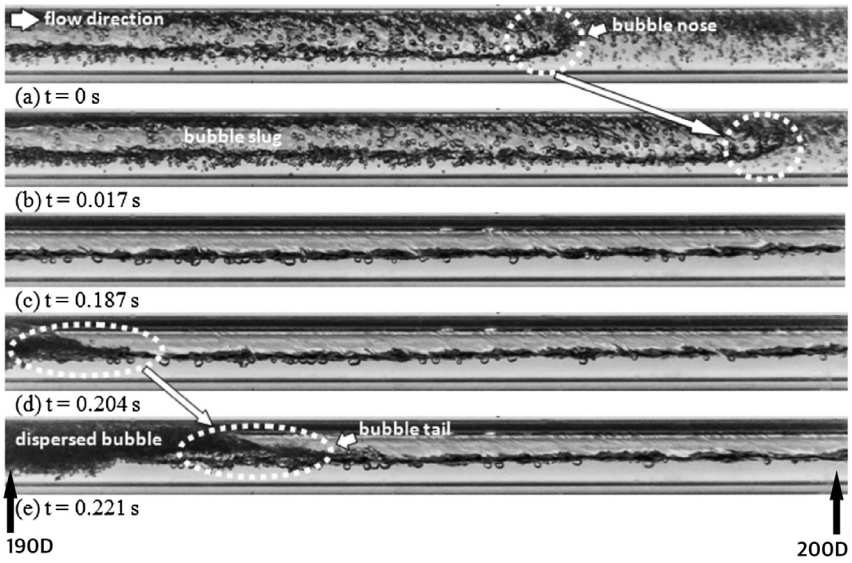

Fig. 14. Snapshot of the developed slug flow visualization for high liquid flow at developed section 190 D–200 D (J_L = 0.77 m/s and J_G = 1.88 m/s).

disturbance waves. For medium J_L in the high J_G areas, addressed as the region V, the mechanism of slug flow formation is influenced by the wave coalescence.

The proposed map is then compared to the initiation map from Woods and Hanratty [29] which divided the mechanisms into 3 types. The proposed map introduces those classifications by considering the effects of the disturbance waves. Although there are several differences among those maps, the slug initiation mechanism follow the wave growth and the wave coalescence for medium and high J_L ($J_L \geqslant 0.10$ m/s). However, this proposed map shows an apparent border that classify each mechanism.

Fig. 17 addresses the onset of slugging criteria as the function of gas and liquid superficial velocities. From the obtained visualization results, the transition from stratified to slug flow is started when J_L = 0.08 m/s to slightly above 0.10 m/s, depending on the J_G. The higher J_G, the higher J_L obtained for the onset of slugging. For the lower J_G ($J_G \leqslant 2.50$ m/s), the proposed onset of slugging criteria is higher than Lin and Hanratty [14], Andritsos et al. [3], and Thaker and Banerjee [24]. This phenomenon differs for the higher J_G. However, the criteria proposed by Woods and Hanratty [29] is higher at the low J_G but lower than the proposed criteria from J_G = 3.00 m/s to 5.00 m/s.

3.2. Pressure measurement

Pressure fluctuations can be used to predict the slug initiation mechanism [12,6]. Measurement of pressure fluctuations were used to verify the slug flow characteristics. Fig. 18 represents the pressure fluctuations at the low J_G and J_L, where J_L = 0.10 m/s and J_G = 2.83 m/s, as the example. At 25 D and 50 D, the static pressure fluctuations are higher than that of 75 D. Visual observation (Fig. 4) indicates that the cause of this is due to a temporary blockage occurring in around 25 D and 50 D regions resulting in larger pressure fluctuations but eventually diminishing into a pseudo-slug and collapsing before 75 D reducing the pressure fluctuations.

Fig. 19 shows the pressure fluctuations for J_L = 0.10 m/s and J_G = 6.20 m/s. As can be seen, there is an increase of average pressure for J_G = 6.20 m/s compared to J_G = 2.83 m/s. Similar to the

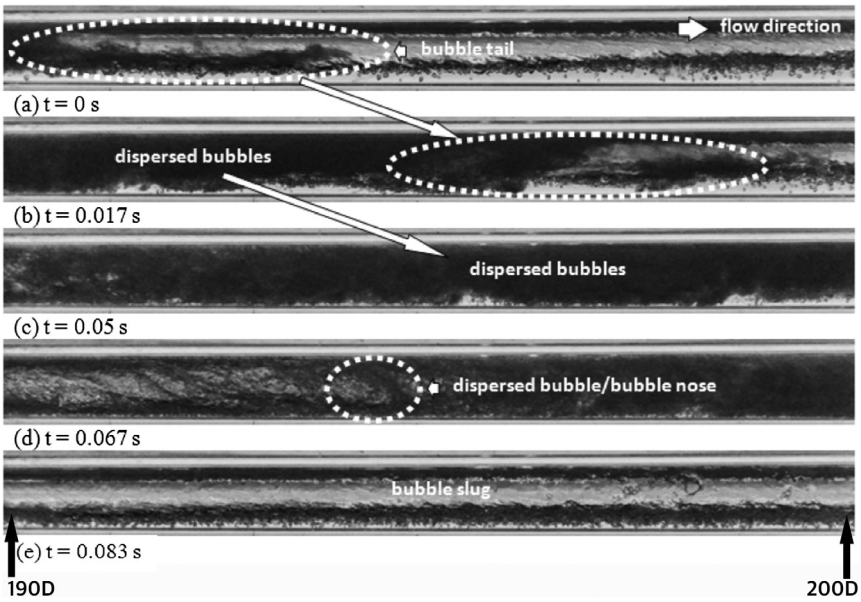

Fig. 15. Snapshot of the developed slug flow visualization for high gas flow at developed section 190 D–200 D (J_L = 0.77 m/s and J_G = 6.2 m/s).

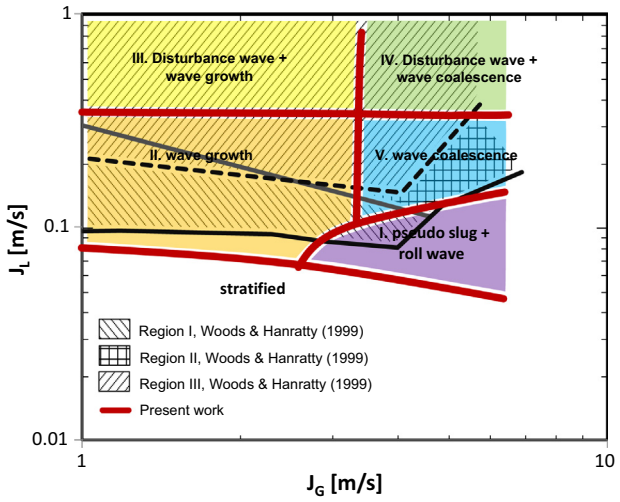

Fig. 16. A proposed flow pattern map for the slug flow mechanism (the results are compared to that of [29]).

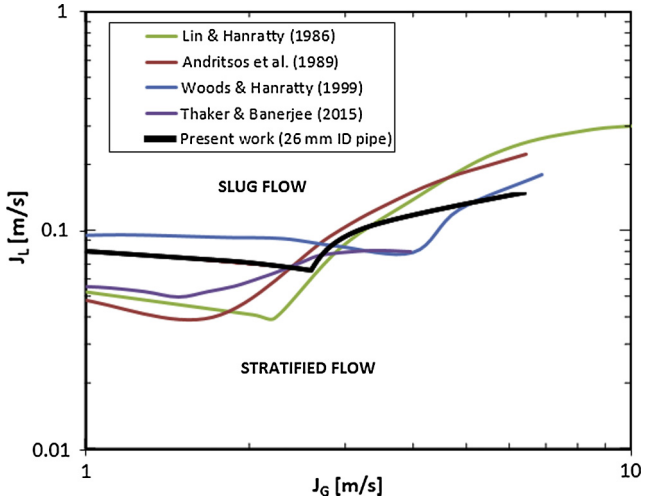

Fig. 17. Transition line from stratified to slug flows.

measurement at J_L = 0.10 m/s and J_G = 2.83 m/s, the pressure fluctuations at 25 D and 50 D were higher than that at 75 D. This is likely due to the waves coalescing around 25 D and 50 D and forming larger waves but reducing and collapsing before 75 D (Fig. 5).

Fig. 20 shows the slug initiation at J_L = 0.31 m/s and J_G = 1.88 m/s. In this figure, the characteristics of pressure fluctuations at 25 D, 50 D, and 75 D are almost similar. This is due to the development of slugs that persist along the length of the pipe as shown in Fig. 6. Thus, reduced pressure oscillations at 75 D as observed for J_L = 0.1 m/s did not occur. The slug initiation characteristics at J_L = 0.31 m/s and J_G = 6.20 m/s also show similar phenomena. However, there is a slight reduction of pressure at 75 D likely due to increased presence of entrainment. Similar to J_L = 0.1 m/s, in higher J_G, the average pressure was higher (see Fig. 21).

Fig. 22 shows the pressure fluctuations at J_L = 0.77 m/s and J_G = 1.88 m/s. In this region, the slug formation is influenced by the disturbance waves and wave growth. As shown in Fig. 8, the disturbance waves trigger the liquid blockage near the air-water inlet, therefore the wave growth occurred. Pressure measurements show that there is a slight difference between the peak pressure times for 25 D, 50 D and 75 D as shown in Fig. 22 as opposed to observations without disturbance waves (Fig. 6) where peak pressures tend to coincide between each location (Fig. 20). It indicates that the presence of disturbance waves and the wave growth exists along the pipe at the initiation section.

Fig. 23 represents the pressure fluctuations at J_L = 0.77 m/s and J_G = 6.20 m/s. The average pressure measurement between 25 D, 50 D and 75 D is similar. Here, a liquid blockage exists at 75 D, indicated the slug formation primarily induced by wave coalescence (Fig. 9). However, again, as the slugging mechanism is induced by disturbance waves in addition to wave coalescence there is a timing difference between peak pressures at each location. The pressure fluctuations are more frequent compared to J_L = 0.77 m/s and J_G = 1.88 m/s as there is presence of dispersed bubbles within the slug flow, as shown in Fig. 9.

The slug initiation phenomena at the developed region (210 D) for various the different J_L and J_G are shown in Figs. 24–26. Fig. 24

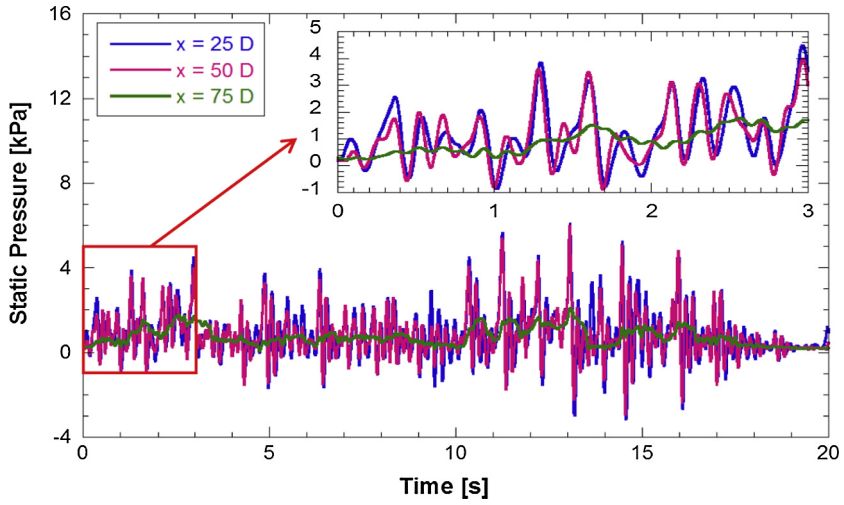

Fig. 18. The pressure fluctuations at a low liquid flow at initiation regions (J_L = 0.10 m/s and J_G = 2.83 m/s).

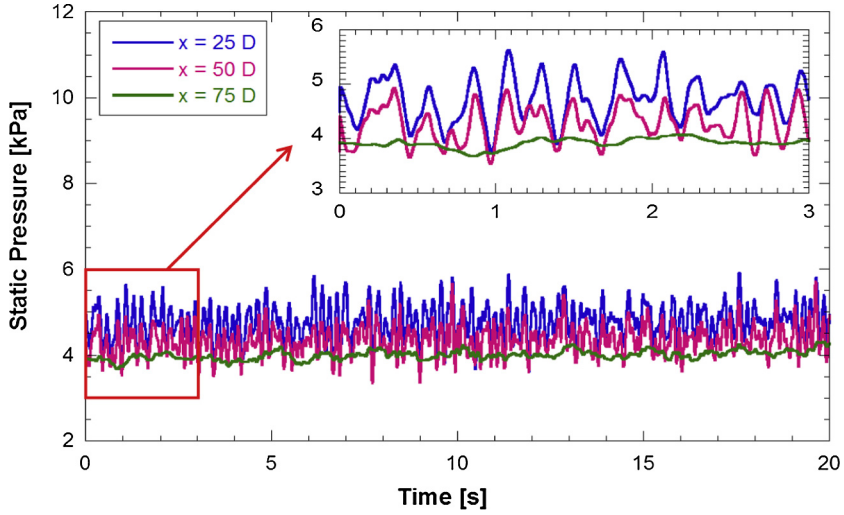

Fig. 19. The pressure fluctuations at a low liquid flow at initiation regions (J_L = 0.1 m/s and J_G = 6.2 m/s).

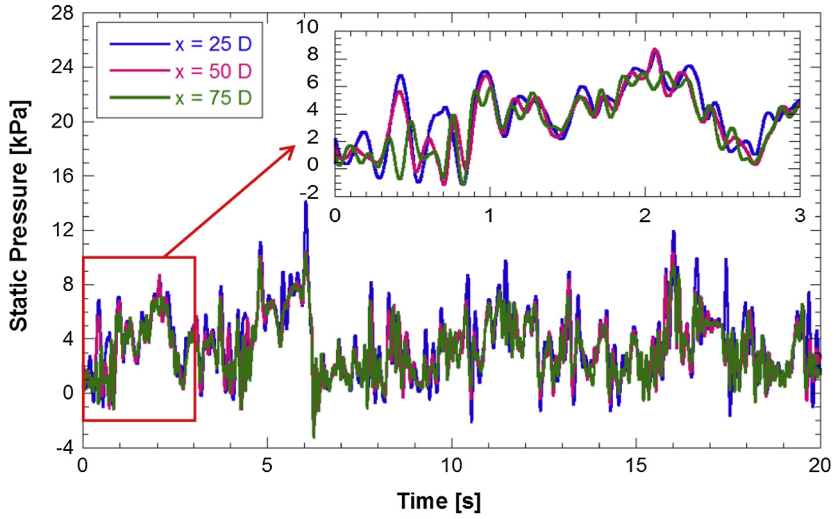

Fig. 20. The pressure fluctuations at a medium liquid flow at initiation regions (J_L = 0.31 m/s J_G = 1.88 m/s).

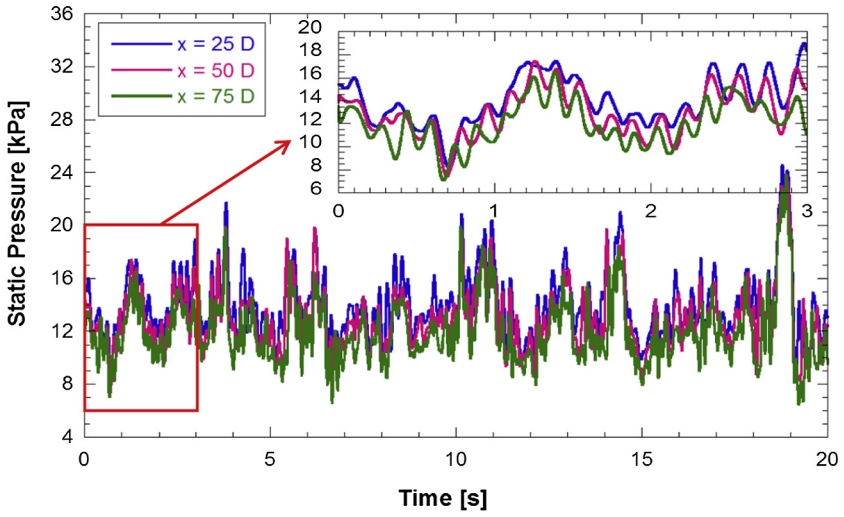

Fig. 21. The pressure fluctuations at a medium liquid flow at initiation regions (J_L = 0.31 m/s and J_G = 6.2 m/s).

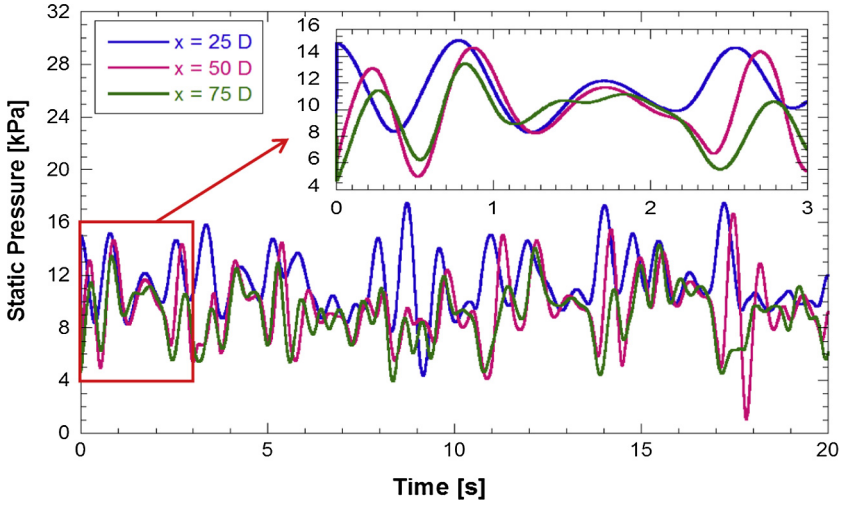

Fig. 22. The pressure fluctuations at a high liquid flow at initiation regions (J_L = 0.77 m/s and J_G = 1.88 m/s).

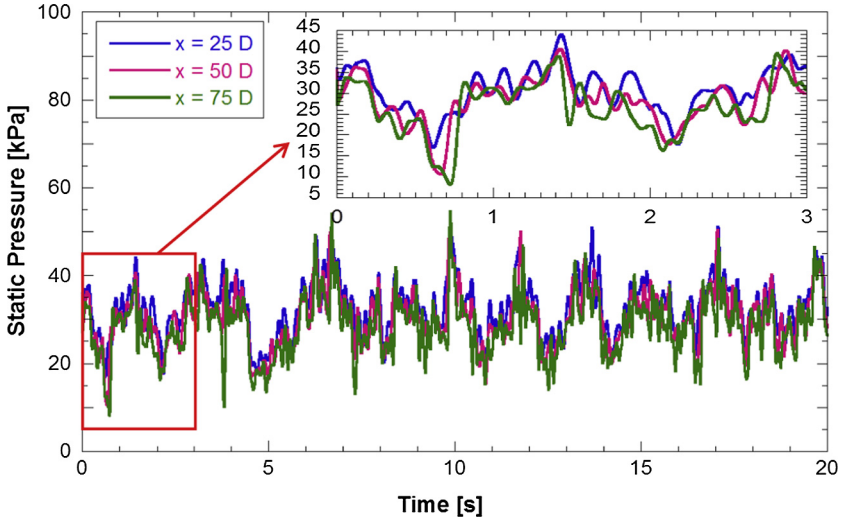

Fig. 23. The pressure fluctuations at a high liquid flow at initiation regions (J_L = 0.77 m/s and J_G = 6.2 m/s).

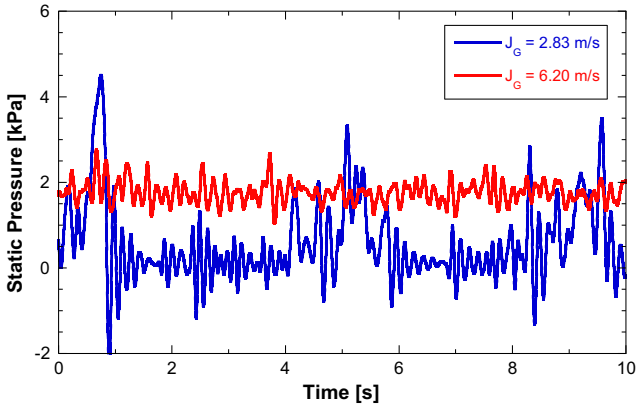

Fig. 24. The pressure fluctuations at $J_L = 0.1$ m/s at developed region (210 D).

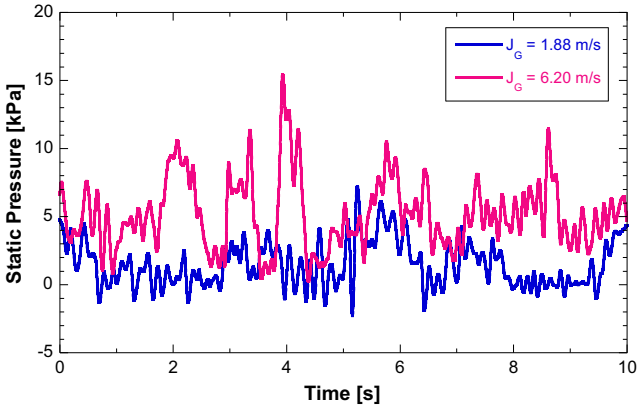

Fig. 25. The pressure fluctuation at $J_L = 0.31$ m/s at developed region (210 D).

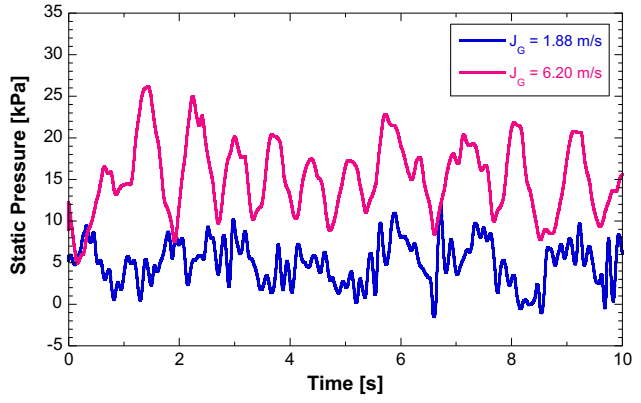

Fig. 26. The pressure fluctuation at $J_L = 0.77$ m/s at developed region (210 D).

shows the pressure fluctuations at lower liquid superficial velocity ($J_L = 0.10$ m/s). For $J_G = 2.83$ m/s, a leap in pressure occurs. This is due to the presence of blockage in the form of pseudo-slugs within the developed section as observed in Fig. 10. When J_G is increased to $J_G = 6.20$ m/s, the pseudo-slug fails to be formed thus resulting in a relatively uniform pressure fluctuation. Moreover, the pressure characteristics were also in a good agreement with the visual observation results, as shown in Figs. 10 and 11.

Fig. 25 shows the pressure fluctuations for the developed slug flow in a higher J_L ($J_L = 0.31$ m/s). The static pressures fluctuate for both $J_G = 1.88$ m/s and $J_G = 6.20$ m/s with occasional leaps in pressure. The presence of slugs in the developed section is confirmed in Figs. 12 and 13. Compared to $J_L = 0.10$ m/s, for $J_L = 0.31$ m/s, the average pressure difference between the $J_G = 1.88$ m/s and $J_G = 6.20$ m/s trials was larger. This difference between average pressure was shown to increase even further for or $J_L = 0.77$ m/s as shown in Fig. 26. For $J_L = 0.77$ m/s and $J_G = 6.20$ m/s, also observed in the developed section are a very large amount yet uniform presence of dispersed bubbles within the liquid slugs (Fig. 15) resulting in a regular pressure leaps with less frequent fluctuations than for $J_L = 0.77$ m/s and $J_G = 1.88$ m/s (Fig. 26). The more frequent fluctuations in for and $J_G = 1.88$ m/s are likely due to the less densely occurring dispersed bubbles (Fig. 14).

3.3. Slug initiation frequency

Figs. 27–29 show the number of new slug formation per second (slug initiation frequency) in relation to the position along the pipe. In the present study, the number of liquid blockage where first time occurred was observed by the high-speed cameras and defined as the initiated slug.

Fig. 27 shows the observation at low liquid superficial velocities where $J_L = 0.31$ m/s. The gas slugs were initiated between 48 D and 58 D, 38 D and 50 D, 28 D and 40 D, and 5 D and 20 D for J_G values of 0.94 m/s, 1.88 m/s, 2.83 m/s, and 3.77 m/s, respectively. When the gas velocity was increased slugs tend to initiate closer to the inlet.

Fig. 28 shows the distribution of slug initiation frequency for a higher J_L of 0.44 m/s. The slug flows were formed between 48 D and 60 D for the low gas superficial velocity of $J_G = 0.94$ m/s. At $J_G = 3.77$ m/s, slug flows were initiated at 8–20 D from the inlet. As J_G increased, the formation of slugs occurred closer to the inlet, similar to the observation for $J_L = 0.31$ m/s. A similar result is obtained for $J_L = 0.77$ m/s where the slug initiation position shifts closer to the inlet with higher values of J_G.

Comparing Figs. 27–29, it can be seen for each case, slugs are initiated at a closer to the inlet position as the J_G increases. However, the effect of liquid superficial velocity on the slug initiation position has a minor effect compared to the effect of the gas superficial velocity. In the present study, slug flow was possible to be initiated at below 40 D. The slug formation can also occur at below 10 D when the J_G was sufficiently high ($J_G = 3.77$ m/s) and J_L was sufficiently low. It is different with the result of Woods and Hanratty [29] where the slug initiation are not formed before 40 D. This is possible due to the inner diameter used in the present study smaller than that of used by Woods and Hanratty (inner diameter 76.3 mm), thus allowing the liquid to more easily block the whole inner pipe diameter.

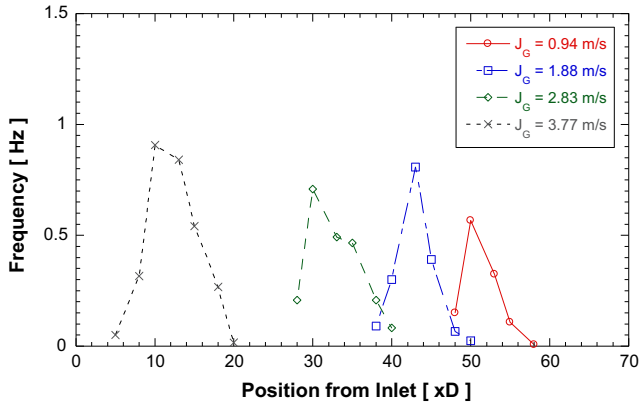

Fig. 27. The distribution of slug initiation position ($J_L = 0.31$ m/s).

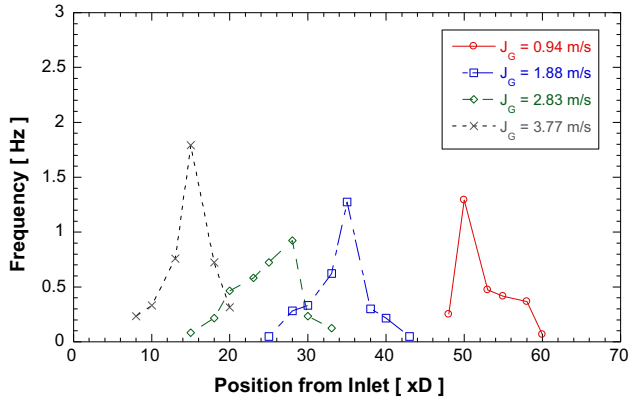

Fig. 28. The distribution of slug initiation position (J_L = 0.44 m/s).

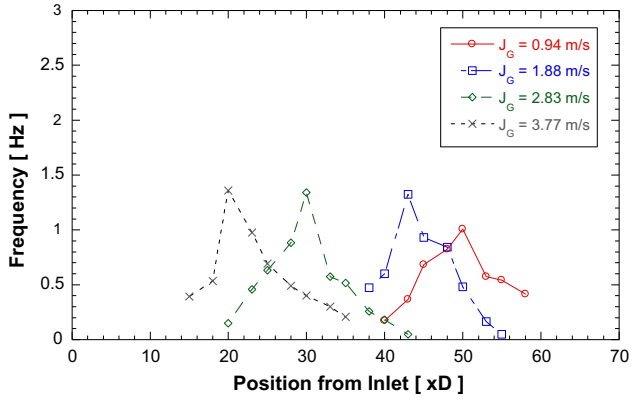

Fig. 29. The distribution of slug initiation position (J_L = 0.77 m/s).

3.4. Evolution of the passing slug frequency along the pipeline

Figs. 30–32 show the effects of gas and liquid superficial velocities on the passing slug frequency in relation to the position along the pipe length. Fig. 30 indicates that the passing slug frequencies initially rise from the position of 25 D and reach the peak at 50 D for J_G = 1.88 m/s and J_L = 0.77 m/s, 0.44 m/s, and 0.31 m/s. For J_G = 1.88 m/s and J_L = 0.20 m/s, the slug frequency also gradually rises at 25 D but reach the peak at 75 D. For J_G = 3.77 m/s, the passing slug frequencies sharply rises from the position around the inlet and reach the peak at 25 D for J_L = 0.77 m/s, 0.44 m/s, 0.31 m/s, and 0.20 m/s, as shown in Fig. 31. In both figures, after reaching the peak, there is a rapid decline of slug frequency, followed by a gradual decrease in slug frequency due to the slug coalescence or collapse and establishment of developed slug flow.

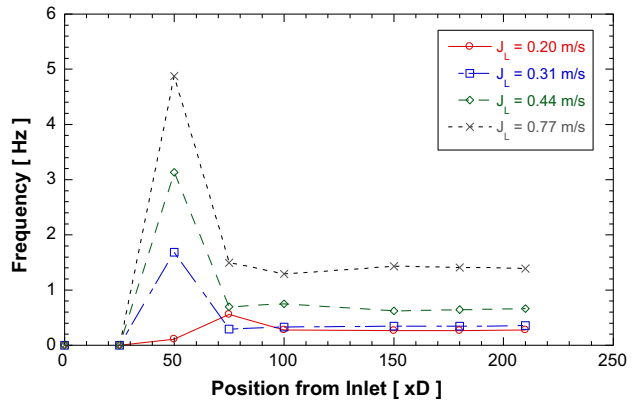

Fig. 30. The effects of J_L to the evolution of passing slug frequency along the pipe (J_G = 1.88 m/s).

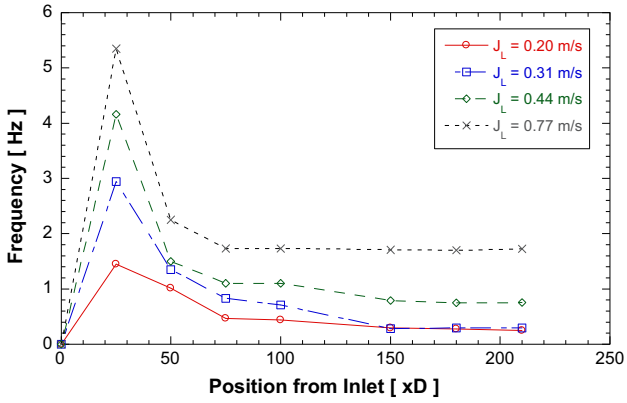

Fig. 31. The effects of J_L to the evolution of passing slug frequency along the pipe (J_G = 3.77 m/s).

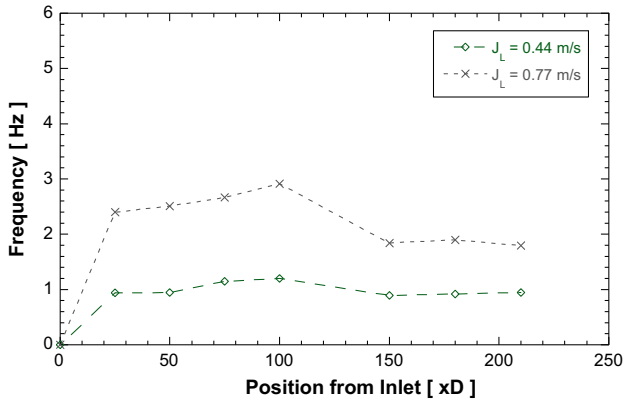

Fig. 32. The effects of J_L to the evolution of passing slug frequency along the pipe (J_G = 6.2 m/s).

At the high J_G of 6.20 m/s, it is clearly observed that the higher J_L contributes to result the larger slug frequency, as presented in Fig. 32. At around first measuring point, a number of slugs are observed, then the slug frequency rises moderately to the highest peak from 25 D to 100 D. In this figure, more slugs are formed and move to the developed test section for the higher J_L. The presence of disturbance waves (presented in high J_L) also plays an important role to produce more slugs. Here, again, slug decay and the recovery of developed slug frequency become the reason of a gradual reduction in slug frequency from the position of 100 D. These observations are also in an agreement with the experimental results from Ujang et al. [25]. Moreover, the developed slugs are then formed after the position of 150 D, for all cases of J_G = 1.88 m/s, 3.77 m/s, and 6.20 m/s, indicated by the steady trend of the slug frequency.

Results of passing slug frequency at the developed test region (210 D) are shown in Fig. 33. As shown in the figure, the slug frequency also increases as the J_L increases. Meanwhile, for J_G less than 3.77 m/s, the observed frequency decreases as the J_G increases. The slug frequency tends to increase as the J_G increases after $J_G \geqslant 3.77$ m/s. It indicates that the slug initiation mechanism between low and high J_G differed each other. The obtained results were also in good agreement with that of Fan et al. [7] and Woods et al. [30].

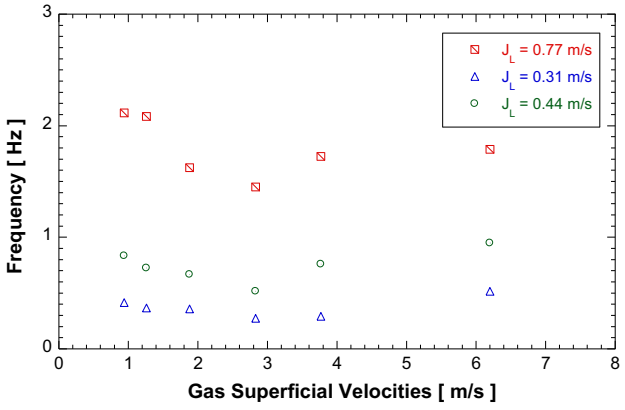

Fig. 33. Slug frequency at 210 D.

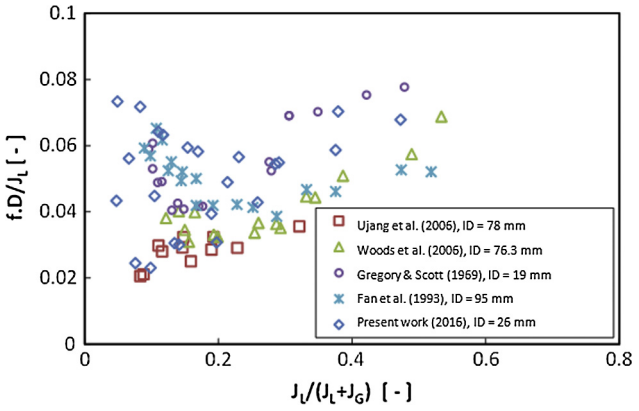

Fig. 34. The comparison of slug frequency at 210 D between the present work and the available previous works.

Fig. 34 shows the comparison of the slug frequency obtained from the present study and the results from Fan et al. [7] and Ujang et al. [25]. A modified Strouhal number which involves slug frequency (f), inner pipe diameter (D), and liquid superficial velocity (J_L) is used to compare the present results to the available previous studies. The slug frequency was taken at 210 D from the inlet. This diagram implicitly shows that liquid flow rates and pipe diameter has a strong contribution on the slug frequency. It can be seen in Fig. 34, that the present experimental data are in close agreement with the experimental data. Nevertheless, the results discrepancies and contradictions among each other studies still occur. Therefore, the studies on the slug frequency will be still an open topic for the future work.

4. Conclusion

An experimental study on the initiation and flow development of gas-liquid slug flow has been conducted with air and water as working fluids and an inner pipe diameter of 26 mm. The liquid superficial velocities (J_L) and gas superficial velocities (J_G) were shown to play an important role in the slug flow initiation and development. The results can be summarized as follows:

1. At very low J_L and high J_G, pseudo-slugs or roll waves occurred. Observation shows that these pseudo-slug or the roll waves were formed by the wave coalescence.
2. At the medium J_L and low J_G, the slug flows initiated under the wave growth mechanism or the Kelvin-Helmholtz instability. Meanwhile, at high J_G, the slug flows were formed by the irregular wave coalescence.
3. At J_L above than 0.35 m/s, the large disturbance waves near the inlet contributed to give the significant effects on the slug flow initiation. At this stage, the slug formations were developed by the disturbance waves in addition to the wave growth and wave coalescence mechanisms for low J_G and high J_G respectively.
4. When J_G increases with a constant J_L, slug flows were formed at the closer position to the inlet. However, the effect of liquid superficial velocity on the slug initiation position has a minor effect compared to the effect of the gas superficial velocity.
5. From low to medium J_G, at the slug initiation position, the frequency of slug occurrence is highest. As the slug flow downstream, number of slugs gradually decrease due to coalescence or collapse. The slug occurrence frequency eventually reaches a stable value downstream where only persisting slugs exist. The liquid superficial velocity plays a significant role in establishing the slug frequency.

Acknowledgement

This present work was carried out within a research project funded by Directorate General of Higher Education, Ministry of Education and Culture, Republic of Indonesia. The project number is LPPM-UGM/1448/LIT/2013. The authors would like to express their sincere appreciation for technical support from Rr. P. Kiranaratri, D. Gunawan, and T.F. Sinaga.

References

[1] E. Al-Safran, Investigation and prediction of slug frequency in gas/liquid horizontal pipe flow, J. Petrol. Sci. Eng. 69 (2009) 143–155.
[2] P. Andreussi, A. Minervini, A. Paglianti, Mechanistic model of slug flow in near-horizontal pipes, AIChE J. 39 (8) (1993) 1281–1291.
[3] N. Andritsos, L. Williams, T.J. Hanratty, Effect of liquid viscosity on the stratified-slug transition in horizontal pipe flow, Int. J. Multiph. Flow 15 (1989) 877–892.
[4] Deendarlianto, T. Höhne, P. Apanasevich, D. Lucas, C. Vallée, M. Beyer, Application of a new drag coefficient model at CFD-simulations on free surface flows relevant for the nuclear reactor safety analysis, Ann. Nucl. Energy 39 (2012) 70–82.
[5] Deendarlianto, M. Andrianto, A. Widyaparaga, O. Dinaryanto, Khasani, Indarto, CFD studies on the gas-liquid plug two-phase flow in a horizontal pipe, J. Petrol. Sci. Eng. (2016) (in press).
[6] A.R. Kabiri-Samani, S.M. Borghei, Pressure loss in a horizontal two-phase slug flow, J Fluid Eng ASME 132 (7) (2010) 1–8.
[7] Z. Fan, F. Lusseyran, T.J. Hanratty, Initiation of slugs in horizontal gas-liquid flows, AIChE J. 39 (11) (1993).
[9] G. Hanyang, G.U.O. Liejin, Experimental investigation of slug development on horizontal two-phase flow, Chin. J. Chem. Eng. 16 (2) (2008) 171–177.
[10] U. Kadri et al., International journal of multiphase flow a growth model for dynamic slugs in gas–liquid horizontal pipes, Int. J. Multiph. Flow 35 (5) (2009) 439–449.
[11] A. Kawahara, P.M.Y. Chung, M. Kawaji, Investigation of two-phase flow pattern, void fraction and pressure drop in a microchannel, Int. J. Multiph. Flow 28 (2002) 1411–1435.
[12] P.Y. Lin, T.J. Hanratty, Detection of slug flow from pressure measurements, Int. J. Multiphase Flow 13 (I) (1987) 13–21.
[13] P.Y. Lin, T.J. Hanratty, Effect of pipe diameter on flow patterns for air–water flow in horizontal, Int. J. Multiphase Flow 13 (4) (1987) 549–563.
[14] P.Y. Lin, T.J. Hanratty, Prediction of the initiation of slugs with linear stability theory, Int. J. Multiphase Flow 12 (I) (1986) 79–98.
[15] J.M. Mandhane, G.A. Gregory, K. Aziz, A flow pattern map for gas-liquid flow in horizontal pipes, Int. J. Multiphase Flow 1 (1974) 537–553.
[16] K. Mishima, M. Ishii, Theoretical prediction of onset of horizontal slug flow, ASME. J. Fluids Eng. 102 (80) (1980) 441–445.
[17] A.O. Nieckele, J.E. Carneiro, R.C. Chucuya, J.P. Azevedo, Initiation and statistical evolution of horizontal slug flow with a two-fluid model, ASME. J. Fluids Eng. 135 (2013) 1–11.
[18] Z. Ruder, P.J. Hanratty, T.J. Hanratty, Necessary conditions for the existence of stable slugs, Int. J. Multiphase Flow 15 (2) (1989) 209–226.
[19] A. Sanchis, G.W. Johnson, A. Jensen, International journal of multiphase flow the formation of hydrodynamic slugs by the interaction of waves in gas–liquid two-phase pipe flow, Int. J. Multiphase Flow 37 (4) (2011) 358–368.

[21] A. Soleimani, T.J. Hanratty, Critical liquid flows for the transition from the pseudo-slug and stratified patterns to slug flow, Int. J. Multiphase Flow 29 (2003) 51–67.
[22] Y. Taitel, A.E. Dukler, A model for predicting flow regime transitions in horizontal and near horizontal gas-liquid flow, AIChE J. 22 (1) (1976) 47–55.
[23] Y. Taitel, A.E. Dukler, A model for slug frequency during gas-liquid flow in horizontal and near horizontal pipes, Int. J. Multiphase Flow 3 (1977) 585–596.
[24] J. Thaker, J. Banerjee, Characterization of two-phase slug flow sub-regimes using flow visualization, J. Petrol. Sci. Eng. 135 (2015) 561–576.
[25] P.M. Ujang et al., Slug initiation and evolution in two-phase horizontal flow, Int. J. Multiphase Flow 32 (2006) 527–552.
[26] J. Villarreal, D. Laverde, C. Fuentes, Carbon-steel corrosion in multiphase slug flow and CO_2, Corros. Sci. 48 (2006) 2363–2379.
[27] R.J. Wilkens, D.K. Thomas, C. Park, A simple technique for determining slug frequency using differential pressure, ASME, J. Energy Resour. Technol. 130 (2008) 1–6.
[28] B.D. Woods, T.J. Hanratty, Relation of slug stability to shedding rate, Int. J. Multiphase Flow 22 (5) (1996) 809–828.
[29] B.D. Woods, T.J. Hanratty, Influence of Froude number on physical processes determining frequency of slugging in horizontal gas–liquid flows, Int. J. Multiphase Flow 25 (1999) 1195–1223.
[30] B.D. Woods, Z. Fan, T.J. Hanratty, Frequency and development of slugs in a horizontal pipe at large liquid flows, Int. J. Multiphase Flow 32 (2006) 902–925.
[31] H.-Q. Zhang et al., Slug dynamics in gas-liquid, ASME, J. Energy Resour. Technol. 122 (2000) 14–21.